7.6 How the Clear-Sky Angle of Polarization Pattern Continues Underneath Clouds: Full-Sky Measurements and Implications for Animal Orientation

One of the biologically most important parameters of a cloudy sky is the proportion q of the celestial polarization pattern that is available to the polarization compass of certain animals. This parameter of clear or cloudy skies has largely been ignored in measurements of skylight polarization. Exceptions are the studies of Brines and Gould (1982), who made point-source measurements, and of Labhart (1999), who used an opto-electronic model to draw qualitative conclusions on the important role of q in animal orientation. Using full-sky imaging polarimetry, Pomozi et al. (2001b) measured how q varies under different meteorological conditions.

It is a well-known phenomenon that distant objects near the horizon (e.g. forests or mountains) appear bluish because of Rayleigh scattering of light between the observer and these distant objects (Können 1985; Coulson 1988). The same phenomenon occurs in the air column underneath clouds. If part of this column is lit directly by the sun, the distribution of the angle of polarization α of scattered light originating from the sunlit part of the column is the same as that of the clear sky. It is less well known that the scattering of direct sunlight on the cloud particles results in the same E-vector pattern as that of the blue sky (Können 1985). As a result of these scattering phenomena, the α-pattern underneath certain clouds approximates that of the clear sky. Thus the celestial E-vector pattern continues underneath clouds under certain atmospheric conditions, such as when the air columns beneath clouds or parts of clouds are lit by direct sunlight

- obliquely from above for smaller solar zenith angles,
- from the side as with bright white cumuli, or
- from below as sometimes occurs at dawn and dusk.

Further on, we refer to these illumination conditions simply as "directly lit by the sun". Apart from heavy overcast skies with multiple cloud layers, such conditions occur frequently if the sky is partly cloudy.

Stockhammer (1959) hypothesized as first that the scattering of direct sunlight between clouds and the earth's surface may generate an E-vector pattern that continues the pattern present in the cloudless celestial regions. Brines and Gould (1982) as well as Pomozi et al. (2001b) and Horváth et al. (2002a) showed by measurements, that α is the most stable and predictable parameter of skylight even under a wide range of atmospheric conditions, whereas p, radiance and spectral composition are highly variable and hence less reliable as orientation cues for animals. Furthermore, α of skylight undergoes only minor changes with wavelength, while p is strongly dependent on wavelength, especially in the blue

and UV (Coulson 1988). Gerharz (1977) demonstrated that the polarization of light originating from the horizon of a cloudy sky is due to the scattered light reflected from extended surface features in the foreground.

The clear-sky polarimetric measurements of Pomozi et al. (2001b) were performed in the Tunisian Chott el Djerid when the sky was clear throughout the day. The polarization pattern of the entire clear sky was hourly measured after sunrise. The cloudy-sky polarimetric measurements were carried out at different places and times in Tunisia. From the cloudy-sky polarization patterns those were selected in which the solar zenith angles θ_s were approximately the same as those in the clear skies shown in Figs. 7.6.1A-C, 7.6.2A-C. Each circular map of skylight polarization in Figs. 7.6.1-7.6.3 contains approximately 543000 pixels, i.e. represents approximately 543000 measured numerical values in a given part of the spectrum. Clouds were recognized in the digitized pictures of the sky using the algorithm of Horváth et al. (2002a).

Figures 7.6.1B,C and 7.6.2B,C represent the p- and α-patterns of the clear skies shown in Figs. 7.6.1A and 7.6.2A, respectively, as measured at 450 nm from sunrise to sunset. For comparison, Figs. 7.6.1D,E and 7.6.2D,E depict the theoretical (single-scattering Rayleigh) patterns of p and α for the same solar positions as those in Figs. 7.6.1A-C and 7.6.2A-C. Comparison of the measured and theoretical patterns indicates that, apart from regions near the sun and antisun, the single-scattering Rayleigh theory describes the gross characteristics of the clear sky polarization patterns relatively well:

- p of skylight first increases with increasing angular distance from the sun, reaching its maximum at approximately 90^o from the sun, and then decreases towards the antisun, and
- the E-vector of skylight is approximately perpendicular to the scattering plane determined by the position of the observer, the sun and the point observed.

The most striking differences between the actual and the theoretical patterns are the consequences of the neutral points. However, since in the vicinity of these neutral points p is smaller than the perceptual threshold p_{min} = 5-10% in animals, the neutral points of skylight polarization are biologically irrelevant.

Figures 7.6.1G,H and 7.6.2G,H represent the p- and α-patterns of cloudy skies shown in Figs. 7.6.1F and 7.6.2F, respectively, measured again at 450 nm. We have chosen approximately the same solar zenith angles θ_s as those represented for clear skies in Figs. 7.6.1A-C and 7.6.2A-C. p is strongly reduced in those celestial regions in which clouds appear.

In many cases, the α-patterns suffer only minor distortions when clouds are present. Compare, for example, the E-vector distributions in Figs. 7.6.1C and 7.6.2C with those in Figs. 7.6.1H and 7.6.2H. Depending on the type, thickness and height of the clouds and on the visibility of the sun (whether it is visible or hidden by clouds), the α-pattern that is characteristic for a clear sky largely continues underneath the clouds (e.g. Fig. 7.6.1H rows 1-5 and Fig. 7.6.2H rows 2-7). In certain cases, especially if the sun is close to the zenith, the E-vector

pattern in cloudy sky regions is completely distorted (e.g. Fig. 7.6.1H rows 6, 7 and Fig. 7.6.2H row 1).

It is known from electrophysiological recordings from the polarization-sensitive interneurons in the cricket's (*Gryllus campestris*) medulla that these neurons respond reliably to E-vectors if $p > 5\%$ and that the standard deviation for the reliability of the E-vector measurements of these neurons is approximately $\pm 6.5^o$ for $5\% \leq p \leq 10\%$ and $\pm 4^o$ for $p > 10\%$ (Labhart 1988, 1996). If $p < p_{\text{threshold}} = 5\%$, crickets cannot perceive the skylight polarization. The polarization-sensitive visual system of crickets determines the direction of the sun from the distribution of α of the clear sky ($\alpha_{clear\ sky}$). If in a cloudy region of the sky the angle of polarization α_{cloud} differs considerably from $\alpha_{clear\ sky}$, the use of α_{cloud} will reduce the accuracy of the determination of the sun's direction if $p > p_{threshold}$. Crickets are not confronted with such a reduction in accuracy if the difference between $\alpha_{clear\ sky}$ and α_{cloud} is below a certain threshold $\Delta\alpha_{threshold}$, which is not smaller than the reliability (± 4-6.5^o) of the E-vector measurements of their polarization-sensitive neurons. To summarise: regions of the sky that provide reliable compass information are characterized by $p > p_{threshold} = 5\%$ and/or $|\alpha_{clear\ sky} - \alpha_{cloud}| \leq \Delta\alpha_{threshold} = 4^o$–$6.5^o$.

The variable q gives the proportion of the skylight pattern that can be used by the insect for reliable E-vector orientation. Figure 7.6.3 presents two examples derived in the way described above from row 1 of Figs. 7.6.1A and 7.6.1F. They demonstrate that surprisingly large parts of a cloudy sky can be used by the insect for compass orientation. Increasing the value of $p_{threshold}$ and/or decreasing the value of $\Delta\alpha_{threshold}$ will decrease q. Since for Fig. 7.6.3 $\Delta\alpha_{threshold} = 6.5^o$ was used instead of 4^o, the numerical values of q are slight overestimates, at least for the vision of the cricket.

Pomozi et al. (2001b) also investigated the wavelength-dependency of the E-vector compass under cloudy conditions. Measurements were made in the blue (450 nm), green (550 nm) and red (650 nm) for the clear and cloudy skies portrayed in Figs. 7.6.1A, 7.6.2A, and 7.6.1F, 7.6.2F, respectively. The following results were obtained:

1. Because of the spatial distribution of p, the value of q is smaller in the solar than in the antisolar half of the celestial hemisphere. The clear-skies data (Table 7.6.1, columns A-C in Figs. 7.6.1 and 7.6.2) largely confirm what has long been deduced from atmospheric optics.
2. The greater the amount of haze and/or aerosol concentration, the smaller is p, and hence the smaller is q.
3. In general, in clear skies, q is always very high (> 80%). It is influenced by the spectral content, the solar zenith angle and, of course, the meteorological conditions.
4. The lower the solar elevation, the larger is q.
5. In general, q increases with decreasing wavelength (see rows 5-7 of Fig. 7.6.1 and rows 1-4 of Fig. 7.6.2). This trend can no longer be observed for very small Δq values between the blue, green and red range of the spectrum.

Most importantly, as shown in Table 7.6.2 and in columns F-H in Figs. 7.6.1 and 7.6.2, conclusions 1-5 also hold for cloudy skies. Only if parts of the clouds and the air columns beneath them are not directly lit by sunlight, does q decrease. This can result from a low p (rows 2, 6 and 7 of Fig. 7.6.1 and row 1 of Fig. 7.6.2) and/or from situations in which the α-pattern does not extend into the air columns underneath clouds (row 6 of Fig. 7.6.1 and row 1 of Fig. 7.6.2). The closer the sun to the horizon, the larger the cloudy-sky values of q, because the low solar elevation increases the chance that the air volumes underneath clouds are directly illuminated by the sun. The shorter the wavelength, the larger the q-values underneath the clouds. These conclusions were drawn not only from the examples presented in this chapter but also from quantitative data obtained under a variety of other atmospheric conditions ranging from clear (cloudless) skies through cloudy to completely overcast skies and for solar zenith angles ranging from 15^o to 90^o.

The polarization of light originating from an area of the sky covered by cloud (termed "cloudlight") consists of two components (Fig. 8.6):

- The first originates from the cloud itself. White light illuminating the cloud remains white but becomes partially linearly polarized after scattering on the cloud particles (ice crystals or water droplets).
- The second component is caused by the scattering of light within the air column between the cloud and the observer. This column emits bluish and linearly polarized light.

Apart from very high clouds (higher than approximately 5 km), the intensity of the first component is much greater than that of the second. When the clouds and the atmosphere underneath them are directly lit by the sun (in a partly clouded sky, under thin clouds or in fog), α of cloudlight follows the same geometrical rule as in the case of blue sky. Because of the randomizing effect of multiple scattering within clouds, p of the first component is usually much lower than that of the clear sky. In general, the first component dominates (its intensity is much greater than that of the second component), so the net p of cloudlight is rather low and usually reaches maximal values of approximately 40% at 90^o from the sun (see pp. 40-41 in Können 1985). As there are many different types of clouds, and as p of cloudlight depends on a multitude of factors, p may differ from cloud to cloud: it is usually lower for denser clouds, because of the randomizing effect of diffuse scattering by the cloud particles.

In contrast to ice-clouds, water-clouds are strongly polarized not only at 90^o but also at approximately 145^o from the sun, where p can reach 60%, i.e. potentially higher values than in the background skylight (see pp. 42-43 in Können 1985). At 145^o from the sun, water-clouds are markedly brighter than at other regions in the sky.

If the clouds are not thin and/or parts of them are not directly illuminated by the sun, their polarizational characteristics differ from those discussed above. Under a heavily overcast sky, when the cloud layer is several km thick, the illumination comes more or less from all directions and, hence, p of the clouds is strongly

reduced (see pp. 42-43 in Können 1985). More light will come from the zenith, where the clouds look thinnest, than from the horizon, meaning that the cloudlight will be horizontally polarized. p of this cloudlight reaches maximal values of 10-20% just above the horizon and decreases rapidly towards the zenith, where it is 0%. A similar polarization pattern occurs in fog not illuminated by direct sunlight. When the clouds are very thick and the visibility is poor (e.g. during rain), the illumination is extremely diffuse, so that p of skylight is reduced to zero.

The full-sky imaging polarimetric measurements of Pomozi et al. (2001b) showed that, even though in cloudy skies p may differ markedly from that in a cloudless sky, α does not. Consider, for example, rows 2-7 in Fig. 7.6.2H: the majority of the sky was covered by thin strato-cumulus and stratus clouds, which considerably reduced p, but the α-pattern remained identical to that in the corresponding clear skies (rows 2-7 in Fig. 7.6.2C). In rows 1-5 of Fig. 7.6.1H thicker and lower clouds were present, which totally distorted the p-patterns, but left the α-patterns underneath clouds (Fig. 7.6.1C, rows 1-5) almost unaltered because parts of the clouds were illuminated directly by sunlight. In contrast, in rows 6 and 7 of Fig. 7.6.1H and row 1 of Fig. 7.6.2H the patterns of both p and α were quite different from those of clear skies (Figs. 7.6.1C, rows 6, 7 and Fig. 7.6.2C, row 1), because the sun was hidden by thicker clouds and the clouds were not directly lit by the sun.

On the basis of the physiological properties of polarization-sensitive interneurons recorded by Labhart (1996), one can compute the proportion of the celestial E-vector pattern, that even under cloudy skies, can be exploited for navigation (if compared with the full E-vector pattern under clear-sky conditions). Under all but the most extreme cloud-cover conditions, this proportion is rather large. Hence, clouds decrease the extent of skylight polarization useful for animal orientation much less than hitherto assumed.

It is a rather wide-spread belief that animals using celestial polarization compass can orient themselves solely by means of the polarization pattern of the clear, blue regions of the sky when the sun is not visible. The reason for this is the assumption that the clouds reduce the extent of sky polarization pattern useful for animal orientation by decrasing p and causing large disturbances in α. However, we have seen above that the celestial α-pattern continues below the clouds under certain atmospheric conditions. This phenomenon can apparently help animal orientation, because also the α-pattern underneath clouds enables polarization-sensitive animals to determine the position of the invisible sun, if p of the cloudlight is not lower than the perceptual threshold of the visual system. Hence, not only the α-pattern of clear, blue sky regions, but under certain atmospheric conditions also considerable parts of the α-pattern below clouds can be useful for animal orientation.

Tables

Table 7.6.1. Proportion q (in %) of the polarization pattern of the clear sky useful for cricket navigation at 650 nm (R), 550 nm (G) and 450 nm (B) evaluated from the clear-sky polarization patterns in Figs. 7.6.1A and 7.6.2A. The degree of linear polarization $p > 5\%$. Number of pixels for the entire sky = 543000. The union of overexposed regions of skies studied in the different spectral ranges was not included. (After Table 1 of Pomozi et al. 2001b, p. 2939).

	Fig. 7.6.1A			Fig. 7.6.2A		
row	R	G	B	R	G	B
1	98.2	98.9	98.5	84.2	91.1	93.0
2	99.9	99.9	99.8	87.8	94.5	96.6
3	97.8	98.9	97.7	91.1	97.4	98.6
4	98.5	98.9	98.7	90.2	97.1	97.8
5	90.7	94.3	94.6	98.6	99.6	99.2
6	87.5	92.9	93.1	99.6	99.6	99.6
7	83.6	90.7	92.9	98.7	99.5	98.9

Table 7.6.2. Proportion q (in %) of the polarization pattern of the clear-sky regions and the clouds useful for cricket navigation at 650 nm (R), 550 nm (G) and 450 nm (B) evaluated from the polarization patterns of cloudy skies in Figs. 7.6.1F and 7.6.2F. For clear-sky regions, the degree of linear polarization $p > 5\%$. For cloudy regions $p > 5\%$ and $|\alpha_{clear\ sky} - \alpha_{clouds}| \leq 6.5^{\circ}$, where α is the angle of polarization. Number of pixels for the entire sky = 543000. The union of overexposed regions of skies studied in the different spectral ranges was not included. (After Table 2 of Pomozi et al. 2001b, p. 2939).

	clear sky regions						clouds					
	Fig. 7.6.1F			Fig. 7.6.2F			Fig. 7.6.1F			Fig. 7.6.2F		
row	R	G	B	R	G	B	R	G	B	R	G	B
1	95.5	93.8	77.8	77.1	79.8	83.9	47.6	59.3	62.3	4.2	4.9	16.0
2	52.8	53.9	68.4	89.8	96.6	98.1	12.9	11.1	18.4	11.7	29.5	44.2
3	90.5	93.9	96.0	90.6	95.9	97.6	27.6	32.6	42.6	43.0	51.8	63.7
4	95.2	97.4	99.3	90.8	96.6	97.4	21.8	21.4	29.4	17.0	32.9	60.7
5	94.7	97.5	97.8	95.6	98.6	98.3	19.9	21.6	24.2	61.9	71.1	81.2
6	92.9	94.6	94.1	98.2	99.7	99.8	6.8	8.3	12.9	49.5	57.1	66.8
7	71.7	76.8	86.6	98.5	98.9	98.3	3.1	2.9	9.4	36.6	58.1	71.8

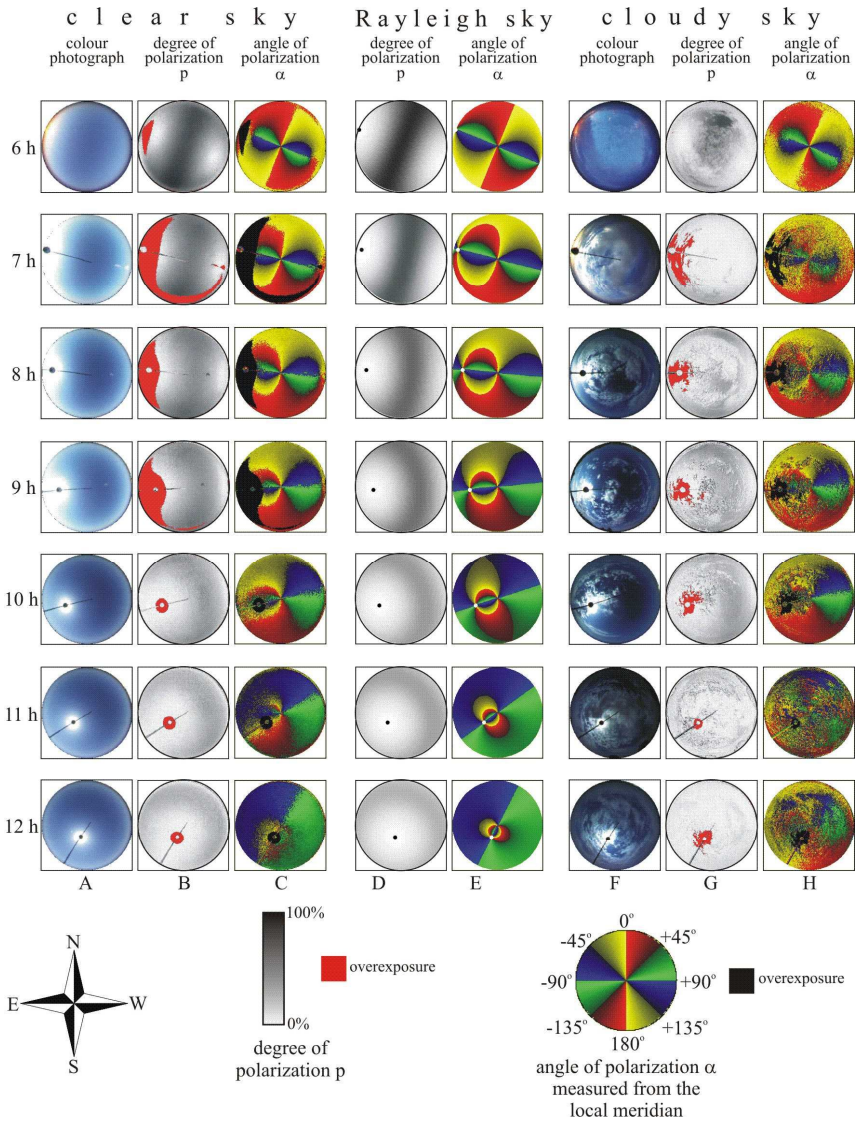

Fig. 7.6.1. A-C: Spatial distribution of radiance and colour, degree of linear polarization p and angle of polarization α (measured from the local meridian) over the entire clear sky measured by full-sky imaging polarimetry at 450 nm for different hourly positions of the sun – from sunrise (06:00 h = UTC+1) to noon (12:00 h) – on 26 August 1999 in the Tunisian Chott el Djerid. D, E: Patterns of p and α of skylight calculated using the single-scattering Rayleigh model for the same solar positions as those in A-C. F-H: Patterns for cloudy skies at different places in Tunisia between 27 August 1999 and 4 September 1999 measured at 450 nm for approximately the same solar zenith angles as those in A-C. The positions of the sun are indicated by dots. The radial bar in the pictures is the wire of the sun occulter. (After Fig. 1 of Pomozi et al. 2001b, p. 2936).

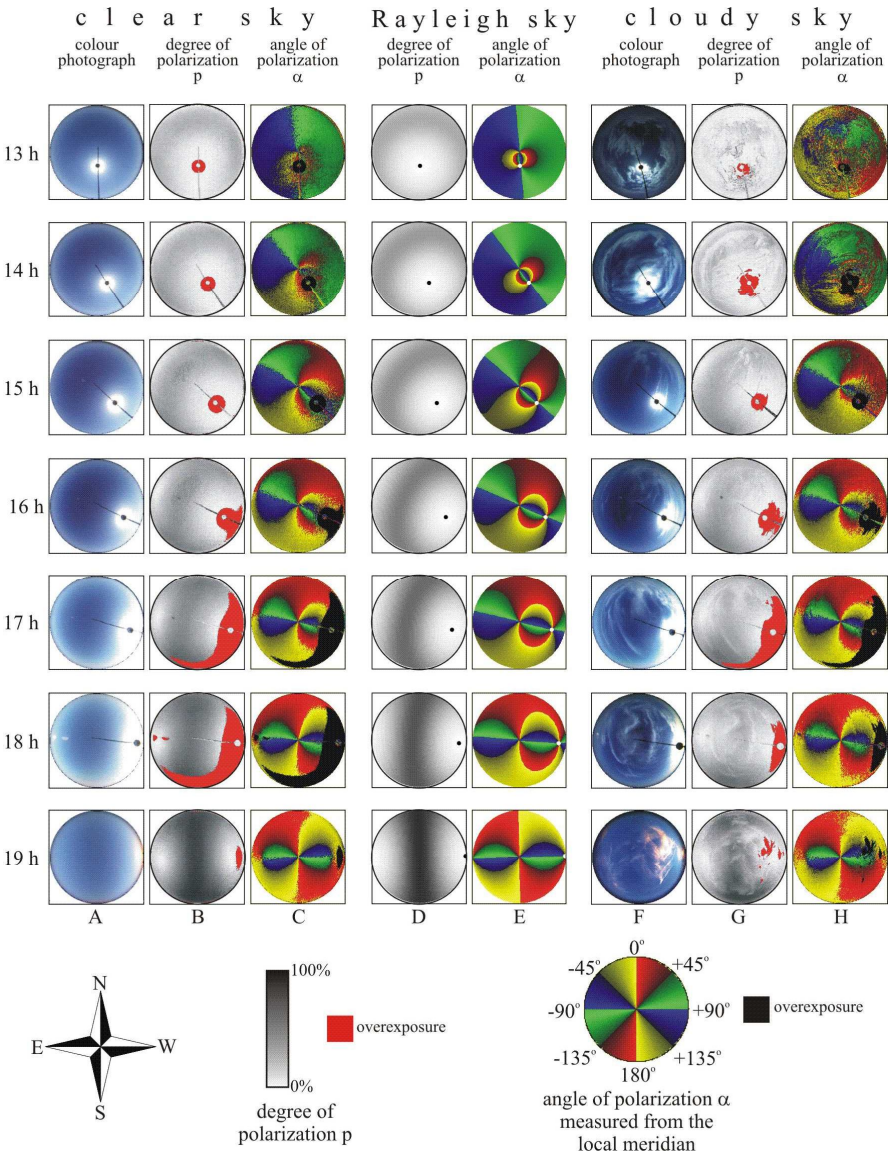

Fig. 7.6.2. As Fig. 7.6.1 from 13:00 h (= UTC+1) to 19:00 (sunset). (After Fig. 2 of Pomozi et al. 2001b, p. 2937).

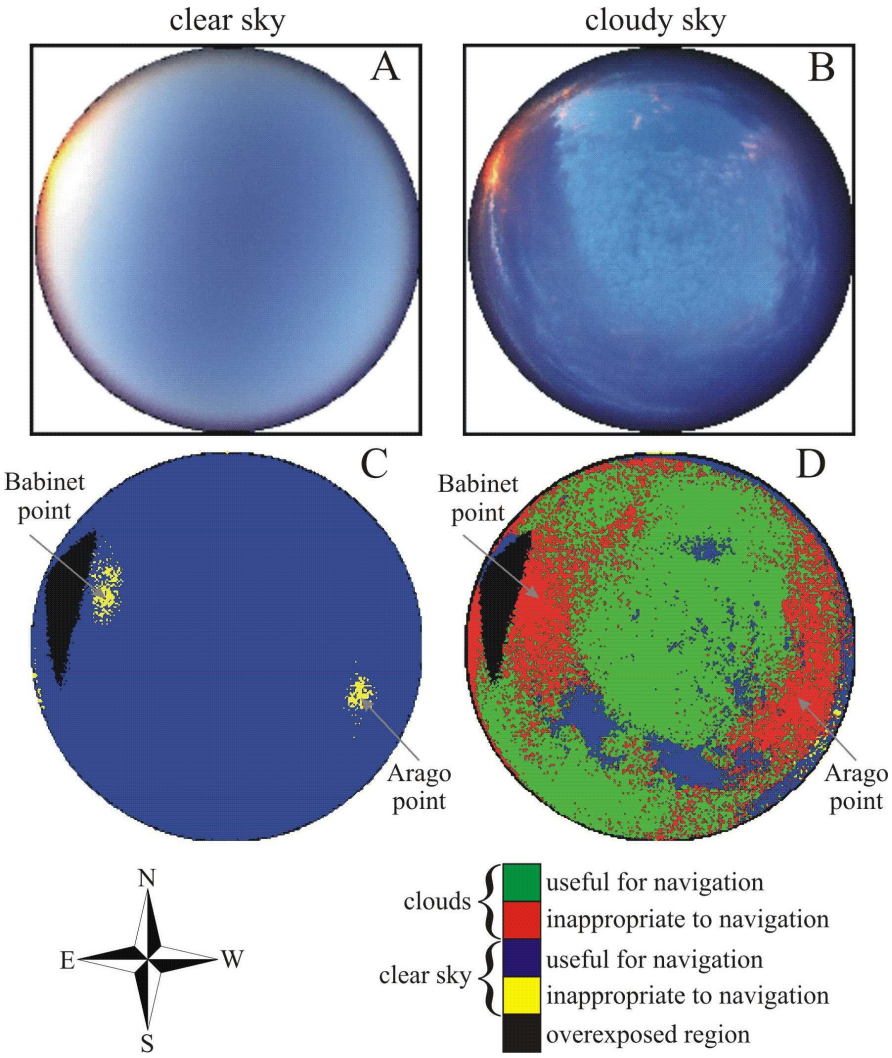

Fig. 7.6.3. The clear (A) and cloudy (B) sky shown in row 1 of Fig. 7.6.1A and in row 1 of Fig. 7.6.1F, respectively. C, D: Regions of the clear (C) and cloudy (D) sky with polarization patterns useful for or inappropriate to reliable cricket navigation calculated on the basis of the celestial polarization patterns measured by full-sky imaging polarimetry at 450 nm. *Blue* (useful for navigation): regions of the clear sky where the degree of linear polarization $p > 5\%$. *Yellow* (inappropriate to navigation): regions of the clear sky where $p \leq 5\%$. *Green* (useful for navigation): regions of the clouds where $p > 5\%$ and $|\alpha_{clear\ sky} - \alpha_{clouds}| \leq 6.5^{o}$, where α is the angle of polarization. *Red* (inappropriate to navigation): regions of the clouds where $p \leq 5\%$ and/or $|\alpha_{clear\ sky} - \alpha_{clouds}| > 6.5^{o}$. *Black*: region of the sky where the photoemulsion was overexposed. The numerical values of p, $\alpha_{clear\ sky}$ and α_{clouds} originate from quantitative full-sky measurements. (After Fig. 3 of Pomozi et al. 2001b, p. 2940).